Supplement of

A temperature- and stress-controlled failure criterion for ice-filled permafrost rock joints

Philipp Mamot[1], Samuel Weber[2], Tanja Schröder[2], Michael Krautblatter[2]

[1]Chair of Landslide Research, Technical University of Munich, 80333 Munich, Germany
[2]Department of Geography, University of Zurich, 8057 Zurich, Switzerland

Correspondence to: Philipp Mamot (philipp.mamot@tum.de)

The supplementary material gives additional information to:

(i) potential error sources, i.e. variations in the ice layer thickness of the samples and the shear rate during the tests (Fig. S1),
(ii) the decreased area of contact between the upper and the lower rock cylinder developing due to shear deformation and considered for the calculation of the peak shear stress (Fig. S2),
(iii) the specific number of performed tests per stress-temperature condition (Table S1),
(iv) the character of time series for shear stress, shear deformation and AE activity at various temperatures (Fig. S3),
(v) the results of AE monitoring (Fig. S4),
(vi) the results of shear stress at failure as a function of temperature (Fig. S5),
(vii) the cohesion and coefficient of friction as a function of temperature (Fig. S6),
(viii) the characteristics of the various failure types (Fig. S7),
(ix) the relationship between failure type and normal stress level (Fig. S8) and
(x) the statistical dispersion measures of the measured peak shear stress values around the calculated failure criterion (Table S2).

Following data (as *.xlsx files) is provided in the zipped folder “Suppl. material”:

- data_acoustic_pdf_Fig. S4
- data_experiments
- data_frictioncoeff_cohesion_Fig. 8
- data_timeseries_acoustic_exp1b_spec4_Fig. S3
- data_timeseries_acoustic_exp2b_spec3_Fig. S3
- data_timeseries_acoustic_exp3b_spec3_Fig. S3

- data_timeseries_acoustic_exp5b_spec2_Fig. S3
- data_timeseries_acoustic_exp5c_spec1_Fig. 5
- data_timeseries_acoustic_exp5c_spec2_Fig. 5
- data_timeseries_acoustic_exp5c_spec3_Fig. 5
- data_timeseries_acoustic_exp5c_spec4_Fig. 5
- data_timeseries_acoustic_exp6b_Fig. 4
- data_timeseries_acoustic_exp6b_spec1_Fig. S3
- data_timeseries_acoustic_exp7b_spec2_Fig. S3
- data_ timeseries_shearmachine_exp1b_spec4_Fig. S3
- data_ timeseries_shearmachine_exp2b_spec3_Fig. S3
- data_ timeseries_shearmachine_exp3b_spec3_Fig. S3
- data_ timeseries_shearmachine_exp5b_spec2_Fig. S3
- data_timeseries_shearmachine_exp6b_Fig. 4
- data_ timeseries_shearmachine_exp6b_spec1_Fig. S3
- data_ timeseries_shearmachine_exp7b_spec2_Fig. S3
- the Supplement text (as *.pdf file) including figures and tables

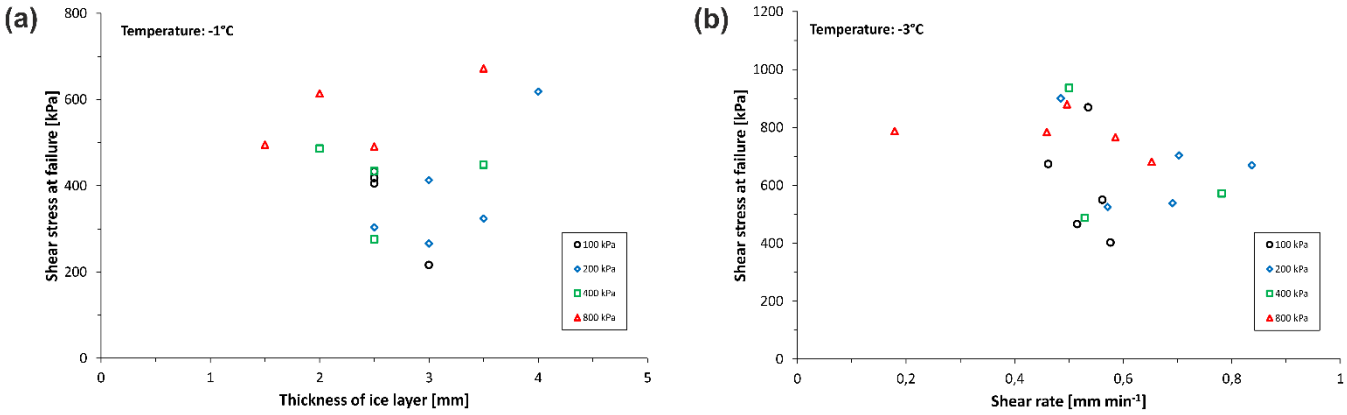

Figure S1: Typical variations in (a) ice layer thickness and (b) shear rate at certain temperatures, both plotted against shear stress at failure and for normal stress levels of 100, 200, 400 and 800 kPa.

Variations in the shear rate (0.3–1.0 mm/min) and in the ice layer´s thickness (1.5–4 mm) were kept low and have no influence on the shear stress at failure (Fig. S1). This is valid for all tested stress and temperature conditions.

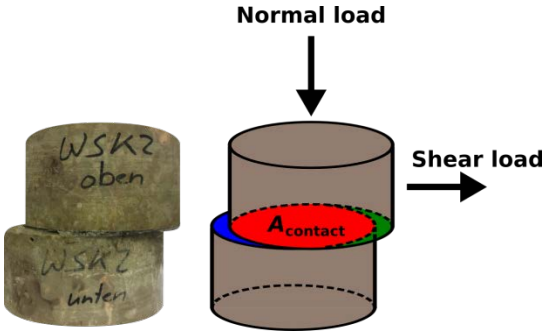

Figure S2: Schematic visualisation of decreasing area of contact $A_{contact}$ between upper and lower rock cylinder during shear experiments.

Normal and shear load as well as normal and shear deformation were recorded during the shear tests and used to calculate normal stress and shear stress considering the changing area of contact $A_{contact}$ which is schematically shown in Fig. S2.

Table S1: Number of experiments per temperature and normal stress condition.

Normal stress class [kPa]	Temperature level [°C]								
	-10	-8	-6	-5	-4	-3	-2	-1	-0.5
100	5	5	5	6	5	5	4	4	4
200	4	4	4	6	5	5	6	5	1
400	5	4	5	5	4	3	5	4	3
800	-	-	-	-	4	5	3	4	4

The number of experiments for each test condition (characterised by a specific temperature and normal stress level) ranged between 1 and 6 (Table S1). The total number of tests was 141.

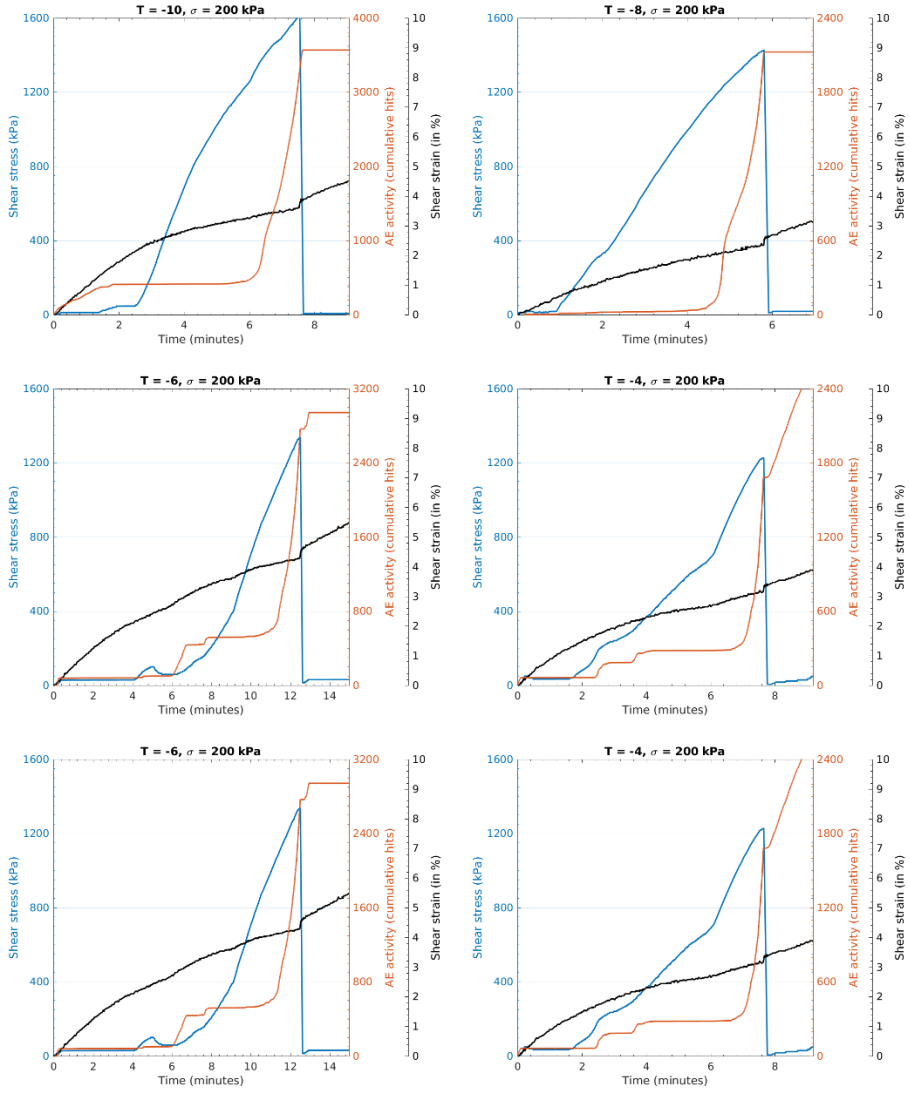

Figure S3: Typical curves of shear stress, shear deformation and acoustic activity for tests applying a normal stress of 200 kPa and various temperatures. All stages of the shearing process (Fig. 4) are depicted including the first part of stage V (post-failure).

Figure S3 displays a selection of representative time series of shear stress, shear deformation and AE activity. Failure is clearly detectable at all presented temperature levels by the peaks in shear stress and their following strong decrease. Furthermore, an increase in cumulative AE hits can be observed just before rupture, pointing to growing microcracks that coalesce and lead to progressive damage. In most of the experiments, the shear deformation reaches one of its maxima at failure. The character of the presented curves corresponds to the demonstrated stages in Fig. 4.

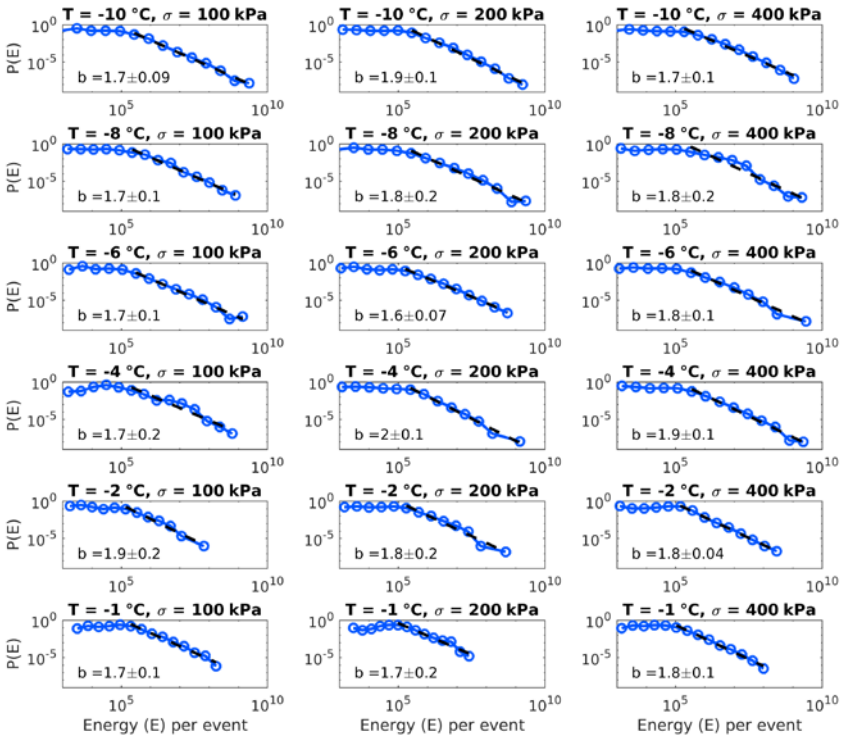

Figure S4: Probability distribution of the event energy for different conditions (temperature and stress level). The power-law function is marked with a dashed black line and its exponent b is given with an error estimation.

The probability density functions (PDFs) of event energy show a power-law behavior spanning 3–5 orders of magnitudes (Fig. S4). The exponent b ranges between 1.6 and 1.9 for the different conditions, but it does not show a relation to temperature or normal load.

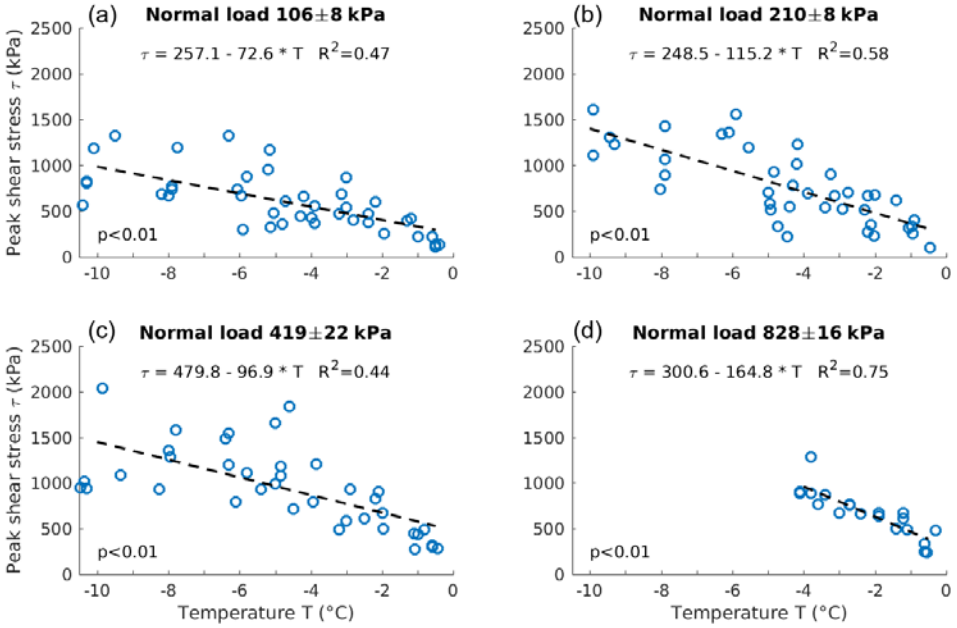

Figure S5: Shear stress at failure as a function of temperature for normal stress levels of 100, 200, 400 and 800 kPa.

At all tested normal stress levels (100, 200, 400 and 800 kPa) the shear stress at failure decreases with increasing temperature (Fig. S5). The calculated total decrease at stresses 100–400 kPa ranges between 63.5 and 78.1 % and refers to a warming from -10 to -0.5 °C. The maximum decrease at 800 kPa measures 60.1 % and refers to temperatures from -4 to -0.5 °C. The measured normal stress means and errors of the tests assigned to a certain normal stress class differ little from the respective class values (maximum 28 ± 16 kPa).

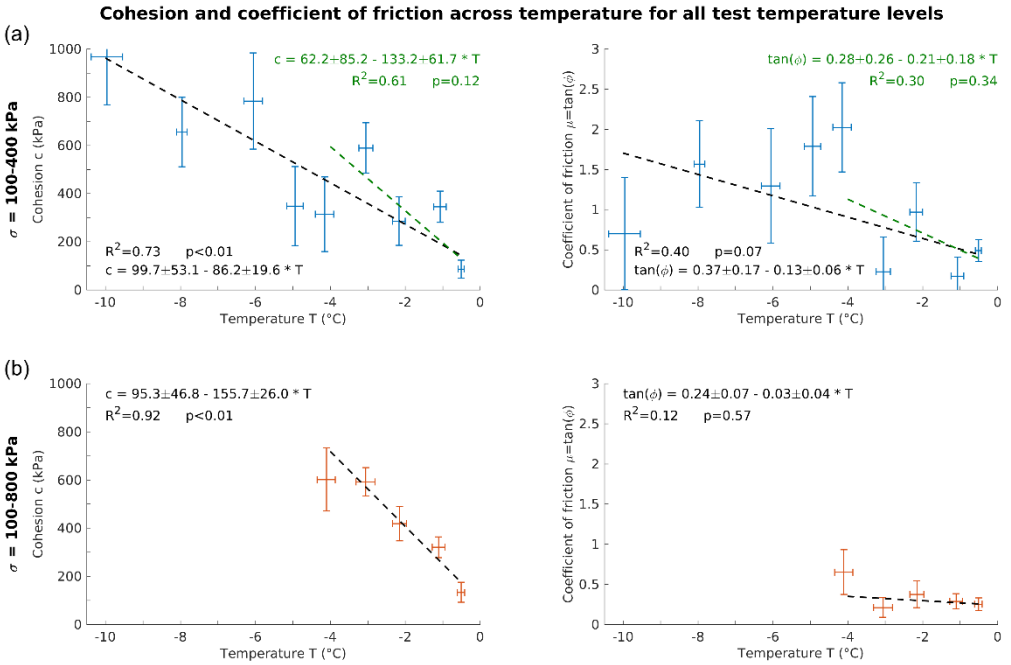

Figure S6: Cohesion and coefficient of friction of ice-filled rock joints as a function of temperature for all tested temperature levels. The crosses display the means and standard deviations of rock temperature and cohesion or friction for the different test temperature classes. (a) Tests at normal stresses 100–400 kPa and temperatures -10 to -0.5 °C (blue crosses). (b) Tests at normal stresses 100–800 kPa and temperatures -4 to -0.5 °C (orange crosses). The dashed lines represent the linear regression functions, which were inversely weighted with the squared standard errors. The green regression lines in (a) refer to a temperature range from -4 to -0.5 °C.

Figure S6 displays the development of formulas for a temperature-dependent cohesion and friction at all tested temperatures. The values of the regression lines correspond roughly to the ones taken for the Mohr-Coulomb failure criterion, which only considers temperature levels with a statistical significance level of $p \leq 5$ % (see Sect. 3.3; Fig. 6). In Fig. S6, R^2-values range between 0.61–0.92 for the cohesion and between 0.12–0.40 for the coefficient of friction. P-values measure 0–12 % for the cohesion and 7–57 % for the coefficient of friction. The ranges depend on the included stress levels and the temperature range tested. The uncertainties presented are higher than the errors of the functions used for the failure criterion (Fig. 7). This justifies the exclusion of tests at certain temperature levels for the development of a robust model.

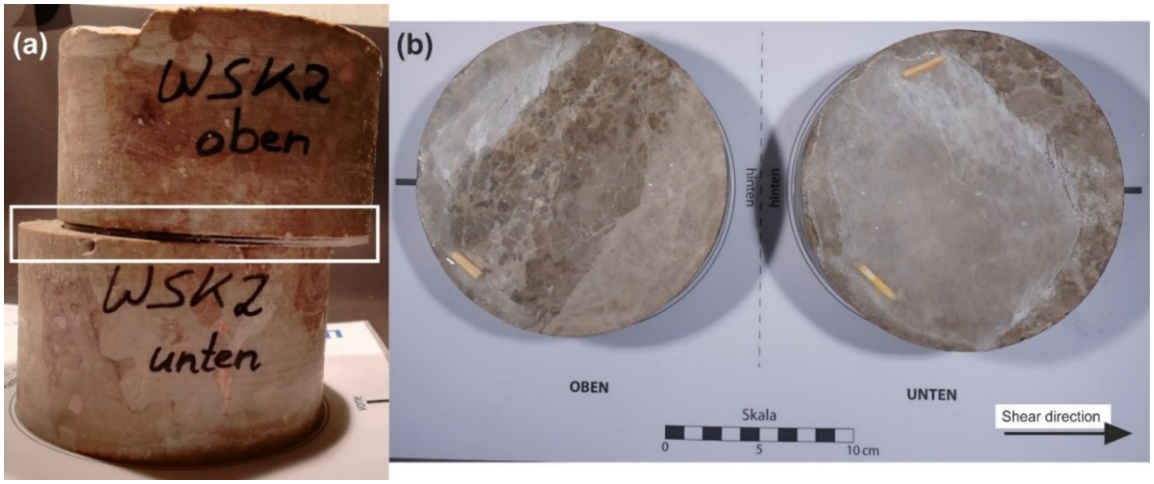

Figure S7: (a) Sheared sandwich sample with fracture along the rock-ice contact. (b) Shear plane after testing with the composite failure type.

Three different types of failure could be identified:

(i) Fracture along the rock-ice interface, where the entire ice infill sticks to the upper rock cylinder (Fig. S7a)

(ii) Fracture within the ice layer

(iii) A composite fracture type of (i) and (ii), where the ice layer broke transversely and was separated so that the rear portion remains at the lower cylinder and the front part sticks to the upper one (Fig. S7b).

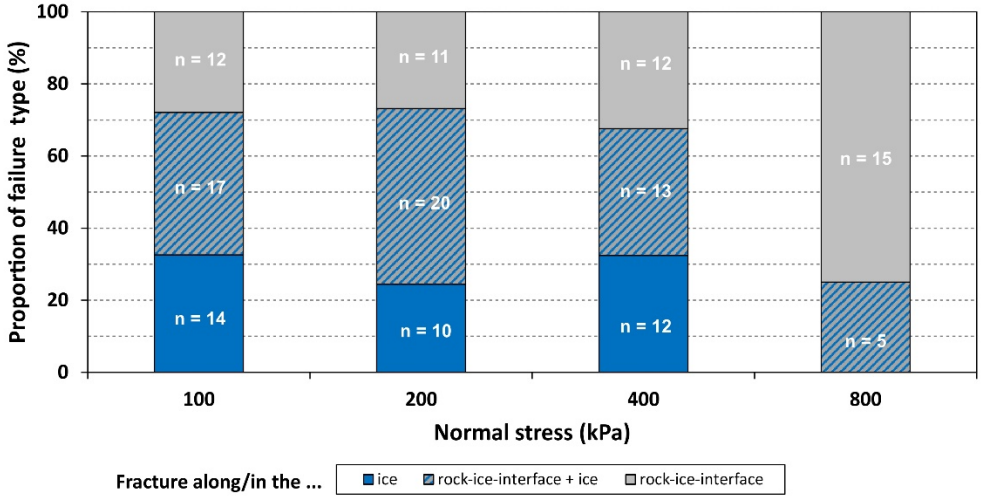

Figure S8: Proportions and absolute numbers of failure types for normal stresses 100–800 kPa and temperatures from -10 to -0.5 °C.

A relationship between failure type and normal stress could not be identified for stress levels 100–400 kPa (Fig. S8). However, at normal stresses of 800 kPa fracturing in the ice did not occur whereas fracturing of rock-ice contacts dominated with 75 %. This overrepresentation of failures along the rock-ice interface may be caused due to the absence of tests at temperatures below -4 °C, where much higher proportions of failures in the ice were observed for tests at ≤ 400 kPa (Fig. 8).

Table S2: Statistical dispersion measures of the measured peak shear stress values around the new derived failure criterion (Fig. 10). Errors calculated for normal stresses 100–400 kPa refer to the valid stress range of the failure criterion. Validation data (V) correspond to temperatures not utilised for the elaboration of the failure criterion. CV = Coefficient of variation. MAD = Mean absolute deviation.

Mean temperature [°C]	σ = 100-400 kPa		Used for model development [C]	Used as validation data for error measurement [V]
	MAD [kPa]	CV [%]		
-0.5 ± 0.1	40.0	19.9	x	
-1.1 ± 0.2	97.5	43.5		x
-2.2 ± 0.2	99.3	24.6	x	
-3.1 ± 0.2	137.8	30.5		x
-4.2 ± 0.2	145.7	19.8	x	
-4.9 ± 0.2	136.4	17.9	x	
-6.1 ± 0.2	206.6	24.6		x
-8.0 ± 0.1	110.4	8.8	x	
-10.0 ± 0.4	252.3	15.0		x

Statistical dispersion measures of the measured peak shear stress values around the failure criterion (Fig. 9) are shown in Table S2. Best accordance is achieved for the shear stress means used for model calibration (correspond to significant temperature levels with p-values ≤ 5 %). The mean absolute deviation (MAD) and coefficient of variation (CV) range between 40–146 kPa and 8.8–24.6 % respectively. The experiments at temperatures -1, -3, -6 and -10 °C (with p-values > 5 %), which had been excluded from the elaboration of the failure criterion, were used for validation. Their shear stress means show higher deviations from the failure criterion, i.e. the MAD and the CV range from 98 to 252 kPa and from 15 to 43.5 % respectively.